COMPRESSED DIGITAL BEAMFORMER WITH ASYNCHRONOUS SAMPLING FOR ULTRASOUND IMAGING

Jun Zhou[1], *Yong He*[2], *Mohan Chirala*[3], *Brian M. Sadler*[4], *and Sebastian Hoyos*[1]

[1]Texas A&M University, [2]University of Texas at Dallas, [3]Samsung Telecommunications America
[4]US Army Research Laboratory

ABSTRACT

The traditional Nyquist sampling architecture does not provide a feasible solution in a large multi-channel ultrasound imaging system. The main issues are the huge data volume after the analog-to-digital interface, high power consumption, and circuit complexity at both the front-end and mid-end. This paper presents a Compressed Digital Beamformer (CDB) framework for the design of an ultrasound imaging system with a large transducer array (≥ 1024) operating at a moderate carrier frequency (≥ 5 MHz). Simulations demonstrate that the proposed CDB framework achieves a Compression Ratio (CR) of 0.1 and Mean Square Error (MSE) of -27.7 dB with 4 quantization bits.

***Index Terms*—**Compressed Sensing, Asynchronous Sampling, Part-Time Randomization, Total Variation, Ultrasound Beamforming.

1. INTRODUCTION

In contrast to other medical imaging methods such as cameras, x-rays, and tomography, ultrasound imaging has several advantages including wide view angle, it is non-invasive, and does not use radiation. The growing use of ultrasound for clinical imaging has motivated the development of portable low cost ultrasound systems without significantly compromising the imaging performance. A state-of-the-art portable ultrasound system integrates a transducer array, a front-end circuit and a signal processing chip, that is typically power supplied by a battery [1] – [3]. The non-intrusive form factor enables daily usage in an open environment. However, portable ultrasound imaging systems suffer from low resolution and high power consumption. According to the imaging theorem, the central carrier frequency determines both the lateral and axial resolution, and the number of transducer elements limits the maximum angular resolution [4]. State-of-the-art portable ultrasound systems typically operate at 2 ~ 4 MHz with less than 32 active transducer elements. The high carrier frequency requires the analog-to-digital converter (ADC) to operate at a high sampling rate to avoid aliasing. When the number of transducer elements is large, the entire data volume at the analog-to-digital interface imposes stringent requirements not only in the circuit power consumption but also the data transmission rate. Moreover, a large transducer array requires dense analog front-end circuitry working in parallel (low-noise amplifier, time-gain controller and ADC). Also, fine timing resolution in a conventional digital beamformer [5], [6] requires either digital interpolation filters or phase rotation calculations. The very high degree of parallelization in silicon must deal with heat dissipation, crosstalk interference, I/O packaging, and other issues.

Various schemes have been suggested to reduce the data volume in ultrasound systems. In [7], the authors compressed the raw RF ultrasound data and/or the baseband data using JPEG and JPEG2000 techniques. This requires Nyquist sampling as the first stage. In [8], the authors demonstrated the feasibility of Compressive Sensing (CS) for the reconstruction of an ultrasound RF signal. However, interpolation filters and/or phase rotation units are required in the mid-end. In [9], the authors proposed a sub-Nyquist sampling architecture by exploiting the finite rate innovation of the ultrasound signal. This system achieves 8-fold data reduction at the expense of a collection of dedicated pre-conditioning filters for each transducer element.

In this paper we present a design of the mixed-signal interface for portable ultrasound systems. A Compressed Digital Beamformer (CDB) supporting a large transducer array (≥ 1024 elements) is proposed for a high central carrier frequency (≥ 5 MHz) portable ultrasound. By converting the amplitude variation into the coded timing information, significant data rate reduction is achieved before beamforming. Simulations show the CDB achieves a compression ratio (CR) of 0.1 and mean square error (MSE) of -27.7 dB when using a quantization level of 4 bits.

The paper is organized as follows. Section II briefly reviews the CS background. Section III introduces the CDB architecture. Section IV presents the Group-based Total Variation (GTV) algorithm tailored for the reconstruction of piecewise-constant signals. Simulations and analysis are given in Section V. Finally, Section VI concludes the paper.

2. COMPRESSED SENSING BACKGROUND

Compressed Sensing (CS) is a framework that enables sub-Nyquist sampling and processing of sparse or compressible signals. According to the CS theorem, any sufficiently sparse or compressible signal can be reliably reconstructed from a much smaller number of incoherent, randomized linear projection samples relative to the full rate Nyquist sampling [10]. One unique advantage of the CS technique is that it integrates sampling and compression into one step, reducing the sampling rate at the analog front-end.

CS adopts a randomized sampling kernel and recovers the signal by solving an l_0-norm optimization problem,

$$\min \|x\|_0 \quad \text{subject to} \quad y = \mathbf{\Phi} x\,, \tag{1}$$

where $\mathbf{\Phi}$ is an $M \times N$ measurement matrix. As shown in [10], problem (1) can be relaxed to an l_1-norm problem when $\mathbf{\Phi}$ satisfies the Restricted Isometry Property (RIP). $\mathbf{\Phi}$ can be derived from Gaussian and symmetric Bernoulli (±1) processes, satisfying the RIP with very high probability [11]. In this paper we use symmetric Bernoulli processes. Many algorithms were developed to solve the l_1-norm problem, such as basis pursuit [12] and greedy approaches [13].

3. COMPRESSED DIGITAL BEAMFORMER

Figure 1 shows the block diagram of ultrasound imaging system with emphasis on the front-end and mid-end circuits. The CDB framework includes an asynchronous sub-Nyquist sampling module, called Digital-assisted Asynchronous CS (DACS) front-end, and a delay-and-sum (DAS) module.

3.1. DACS front-end

Figure 2 shows the DACS front-end. It consists of two parts, a Continuous-Time Ternary Encoder (CT-TE) and algorithmic logic. Suppose the input signal $z(t)$ has been pre-amplified to full-scale with a peak-to-peak value U. V_{ref} is the reference signal. The threshold generator divides U into 2^Q levels based on quantization bit level Q. At each cycle, it provides a threshold pair ($V_{th,L}$, $V_{th,H}$) to the comparator. The difference between $V_{th,L}$ and $V_{th,H}$ is a quantization step L.

Threshold pair ($V_{th,L}$, $V_{th,H}$) forms a comparison window, which is initialized to a running average of the input. When $z(t)$ goes higher than $V_{th,H}$ or lower than $V_{th,L}$, the comparator outputs "+1" or "-1", respectively, and the threshold generator updates the comparison window accordingly to capture the input variation; otherwise, the comparator outputs "0", and the threshold pair remains unchanged. As a result, the signal amplitude variation is modulated onto the ternary timing information. Without loss of generality, we assign unit amplitude to "+1" and "-1" pulses.

The CT-TE scheme differs from other amplitude-to-time conversion schemes, including Time Encoding Machine (TEM) [14], delta modulation [15] and integrate-and-fire methods [16]. Both TEM and delta modulation incorporate a negative feedback which once started, always flip-flops, like a sigma-delta modulator output with constant input, and continues to generate output even with no input signal. The integrate-and-fire scheme also produces an output when no input variation occurs, resulting in signify-cant power overhead. In contrast with the CT-TE scheme an output occurs only when significant input variation occurs.

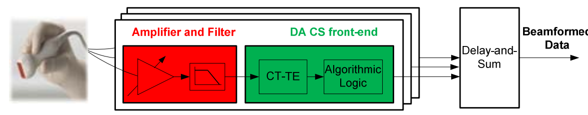

Figure 1. Ultrasound imaging system with emphasis on front-end and mid-end circuitry.

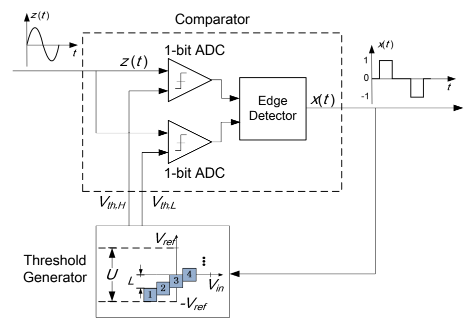

Figure 2. Architecture of the CT-TE scheme.

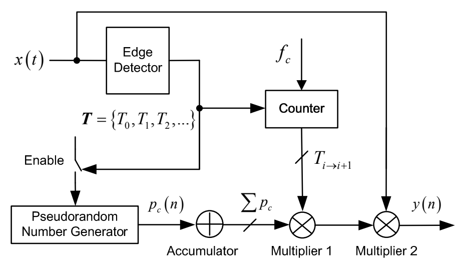

Figure 3. Block diagram of the algorithmic logic.

The output of the CT-TE scheme is ternary piecewise-constant $x(t) = \{-1, 0, 1\}$. A discrete set of times $\boldsymbol{T} = \{T_0, T_1, T_2, \ldots\}$ represent the time instants of each transition edge in $x(t)$. Note that no clock is involved in the CT-TE module. The output is signal-driven and is asynchronous and a continuous function of time.

In this architecture, we are interested in the elapsed time period between the successive transition edges. Let $T_{i\to i+1}$ denote the time between the i^{th} and $(i+1)^{\text{th}}$ transition. $T_{i\to i+1}$ can be calculated by counting the elapsed clock cycles $C_{i\to i+1}$ that runs at a pre-defined frequency f_c,

$$T_{i\to i+1} = C_{i\to i+1}\Delta t \tag{2}$$

where $\Delta t = 1/f_c$. We take f_c to be much higher than the Nyquist rate of the input signal for sufficient timing resolution. Due to the ternary piecewise-constant characteristic, the inner product of a PN sequence with the zero-value sections is trivial. Hence, the PN generator is halted and all timing information for these no-change periods can be modulated to the next nonzero-value, as shown in Figure 3. In this way, an equivalent compact signal $x_{\text{eq}}(n)$ is obtained from $x(n)$,and this is input to the l_1-norm optimization. Then, $x(n)$ is restored from $x_{\text{eq}}(n)$ by demodulating the zero-valued sections. Thus the DACS front-end enables part-time operation of the PN generation and randomization, which are the most power-demanding operations in a conventional CS scheme, such as the random demodulator [17]. Let us define the part-time ratio (PTR) to quantify the percentage of part-time operation,

$$r_{\text{part-time}} = \frac{\sum_{i \in x_{\text{eq}}} T_{i \to i+1}}{\sum_{i \in x} T_{i \to i+1}} \quad . \tag{3}$$

Note that $x_{\text{eq}}(n)$ can be described by the transition edge and section length. This asynchronous edges (AE) approach, by itself, is noise sensitive and generally results in poor reconstruction. Consequently, next we propose a group-based total variation (GTV) scheme to improve the noise robustness, leading to high quality reconstruction while maintaining significant compression.

3.2. Group-based Total Variation

We define a group as a collection of consecutive samples that have the same amplitude. We develop a GTV scheme for sparse recovery from these noise corrupted measurements. The problem is to minimize the objective in (4)

$$J(x) = \alpha \mathrm{TV}(x) + \gamma \mathrm{GTV}(x) + \|y - Ax\|_2^2 \tag{4}$$

$$\mathrm{TV}(x) = \|Dx\|_1$$

$$\mathrm{GTV}(x) = \sum_{i=1}^{N} \left\| Dx_i^{i+g_i-1} \right\|_1 \tag{5}$$

$$g_i = \arg\max_g \left(\left\| Dx_i^{i+g} \right\|_\infty \le TH < \left\| Dx_i^{i+g+1} \right\|_\infty \right)$$

where D is the standard first-order derivative matrix, A is a randomized matrix, and α and γ are tuning parameters balancing the TV and GTV penalties. We denote x_i^j to be the string comprising samples i through j within x, g_i is the group size from the i^{th} sample, TH is similarity threshold.

We adopt the iteratively reweighted least squares (IRLS) method [18] for sparse recovery. As shown in [18], the l_p-norm ($p \ge 1$) can be approximated by the weighted l_2-norm at each iteration step. By accounting for both the TV [19] and GTV, the included piecewise-constant feature expedites the convergence speed. Moreover, the GTV penalty mitigates the noise effect in the piecewise-constant sections. The proposed GTV scheme is given in Algorithm 1.

Algorithm 1: Group-Based Total Variation

INPUT: the randomization matrix $\mathbf{\Phi}$, the received signal y, the threshold TH, the maximal iteration number $imax$, and the tuning parameters α and γ.

OUTPUT: the estimation of piecewise-constant signal $\hat{x}$

PROCEDURE:

1. Initialize the estimated signal $x_{t-1} = 0$, the weight $W_{t-1}^j = 1$ for its jth neighbor, and the iteration count $t = 1$.
2. **while** $t \le imax$, **do**
3. Find the gradient of x, $x' = Dx$.
4. Perform thresholding, find group size for each sample, $g_i = \arg\max_g |x'^{i+g}_i|_\infty \le TH < |x'^{i+g+1}_i|_\infty$.
5. Calculate the weight of the least squares approximation, $W_{\text{total}}(i) = \alpha D' W_{t-1}^1(i) D + \gamma \sum_{j=1}^{g_i} D_j' W_{t-1}^j(i) D_j$,where D_j is j-shifted gradient matrix.
6. Calculate the Least Squares solution for current iteration, $x_t = (\mathbf{\Phi}' * \mathbf{\Phi} + W_{\text{total}})^{-1} * \mathbf{\Phi}' y$.
7. Update the weight of all neighbors, $W_t^j = 2*\mathrm{diag}(1/D_j x_t)$
8. Increment t
9. **end while** and **return** $\hat{x} \leftarrow x_t$

---

4. SIMULATION RESULTS

An ultrasound imaging system with 64 transducer elements is simulated to illustrate the concept. Each channel employs an independent CDB framework. From the sampling and digitization perspective, the system architecture and simulation results are readily extended to a large transducer array ($\ge$ 1024 elements) with proper scaling.

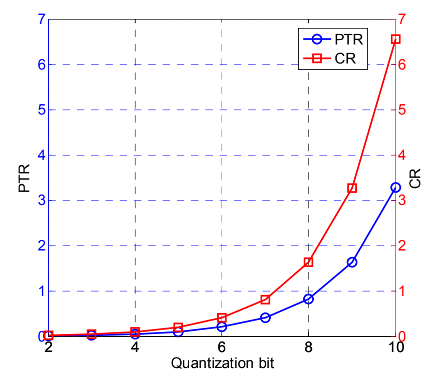

Figure 4. Part-time ratio (PTR) and compression ratio (CR) of the CDB system with different quantization levels.

Figure 4 shows the PTR and CR of the CDB framework with a carrier frequency of 5 MHz. Suppose the Nyquist sampling scheme operates at 11 MHz. The comparison clock rate in the CT-TE module is set to 1.1 GHz, 100 times higher than the Nyquist rate, for sufficient timing resolution. As shown, PTR and CR increase rapidly with Q. When Q is larger than 8, both PTR and CR become larger than 1 due to the oversampling. For Q = 4, the PTR is around 0.048, providing more than 20-fold reduction for operating the randomized measurements, including the PN generator and accumulator modules. Because the total power is linearly dependent on the operating time, the asynchronous-time operation directly lowers the system power. Note that the CR is roughly 0.1 with Q = 4. This implies a 10-fold reduction in data volume compared with Nyquist sampling, implying further significant power reduction. The Gigahertz clocking introduces moderate complexity, although we employ comparators rather than a conventional ADC. Moreover, our approach does not require the conventional digital circuits for fine timing resolution, such as the digital filters in interpolation beamforming [5] or CORDIC units in phase rotation beamforming [6]. These power saving benefits can be applied to a large ultrasound transducer array configuration.

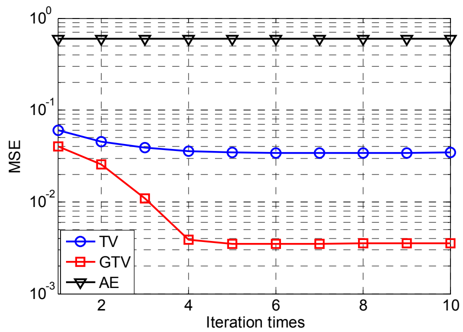

Figure 5. Reconstruction performance of the compressed ultrasound RF signal by the conventional TV method and the proposed GTV scheme.

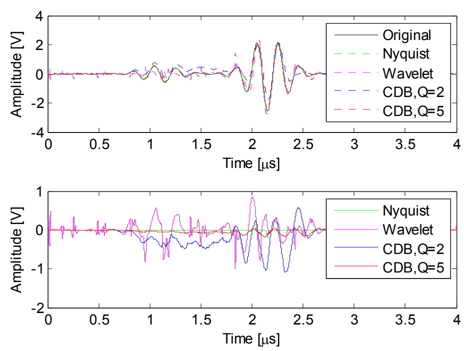

Figure 6. Reconstruction of one scan line after digital beamforming using the proposed CDB framework: (upper plot) reconstructed waveform; (bottom plot) reconstruction error.

Figure 5 compares the RF signal reconstruction of the GTV scheme for one transducer element at 30 dB SNR. Q = 4 and the sub-Nyquist sampling ratio is set to 0.15 in all CS schemes used for comparison. By evaluating the MSE at each iteration, the GTV exhibits better recovery than the AE scheme. Intuitively, randomization in the CDB framework makes the noise evenly distributed across the measurements, whereas the small valued samples in the AE scheme are more sensitive to noise than those with larger values. The CDB framework has faster convergence because the GTV penalty selectively chooses a direction that favors the piecewise-constant characteristics as the minimizer approaches to the optimum. The additional GTV constraint in the cost function expedites the convergence rate and increases the noise robustness.

Figure 6 shows one reconstructed scan line after digital beamforming in the CDB framework. We compare with a Nyquist sampling scheme using 12 bit resolution and the compression scheme in [8] with Daubechies wavelets (db4). Similar to the Nyquist sampling scheme, the CT-TE also introduces quantization error, which can be improved by increasing the quantization level Q. Figure 6 shows that the CDB scheme using 5 quantization bits has better performance than the conventional CS scheme with the wavelet transform, and has a peak error similar to the Nyquist sampling scheme with 12 quantization bits. Note that the relatively larger quantization errors appear near the peaks. In ultrasound imaging the beamformed data is typically compressed by a log function to reduce the dynamic range for display. Hence, the quantization error introduces more undesired visual difference at the boundary of background and tissue when a small Q is employed. This is evident in Figure 7, which shows reconstructed ultrasound images using our proposed CDB framework with the quantization level Q changing from 2 to 5. Comparing to the ideal image, the MSE is -10.8 dB, -16.4 dB, -27.7 dB and -38.3 dB as Q varies from 2 to 5. The edge error effect is well reduced when Q increases to 4.

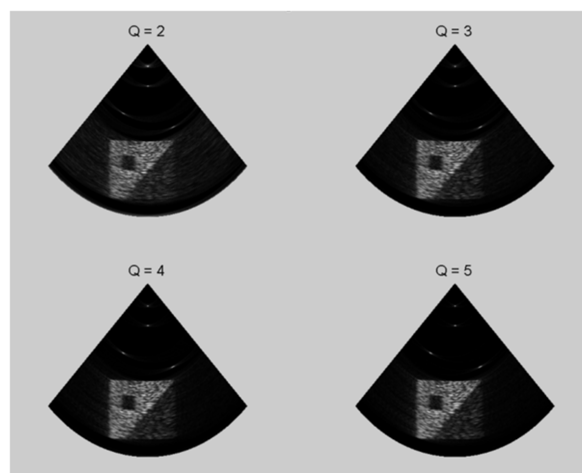

Figure 7. Reconstructed ultrasound images using the CDB framework with different quantization bit Q.

5. CONCLUSION

In this paper we presented a compressed digital beamformer for ultrasound imaging systems. We showed that asynchronous sampling, coupled with GTV reconstruction, can yield results equivalent to a high dynamic range Nyquist rate system with significantly lower hardware complexity.

6. REFERENCES

[1] GE Healthcare, Vscan, https://vscan.gehealthcare.com/gallery/a-quick-look-at-vscan

[2] Siemens, ACUSON P10TM, http://www.medical.siemens.com/webapp/wcs/stores/servlet/ProductDisplay~q_catalogId~e_-1~a_catTree~e_100010,1007660,12761,1005253~a_langId~e_-1~a_productId~e_182941~a_storeId~e_10001.htm

[3] Signostics, Signos Personal Ultrasound, http://www.signosticsmedical.com/home.php.

[4] S. K. Edelman, *Understanding Ultrasound Physics: Fundamentals and Exam Review*, Esp, 2nd edition, June 1994.

[5] K. Karadayi, C. Lee, and Y. Kim, "Software-based Ultrasound Beamforming on Multi-core DSPs," *IEEE International Ultrasonics Symposium*, pp. 503-506, 2011.

[6] A. Agarwal, et. al., "New Demodulation Method for Efficient Phase-Rotation-Based Beamforming," *IEEE Trans. on Ultrasonics, Ferroelectrics and Freq. Ctrl.,* vol. 54, no. 8, pp.1656-1668, 2007.

[7] Y. F. Li and P. C. Li, "Ultrasound Beamforming Using Compressed Data," *IEEE Trans. on Information Technology in Biomedicine*, vol. 16, no. 3, pp. 308-313, May 2012.

[8] D. Friboulet, H. LIebgott, and R. Prost, "Compressive sensing for raw RF signals reconstruction in ultrasound," *IEEE Ultrasonics Symposium*, pp. 367 – 370, 2010.

[9] N. Wagner, Y.C. Eldar, and Z. Friedman, "Compressed Beamforming in Ultrasound Imaging," *IEEE Trans. on Signal Processing*, vol. 60, no. 9, pp. 4643 – 4657, Sept. 2012.

[10] E. J. Candès, M. B. Wakin, "An Introduction to Compressive Sampling," *IEEE Signal Proc. Magazine*, vol. 25, no. 2, Mar. 2008.

[11] J. A. Tropp, J. N. Laska, M. F. Duarte, J. K. Romberg and R. G. Baraniuk, "Beyond Nyquist: Efficient Sampling of Sparse Bandlimited Signals," *IEEE Trans. on Information Theory*, vol. 56, no. 1, pp. 520-544, Jan. 2010

[12] E. Candès, J. Romberg and T. Tao, "Robust uncertainty principles: Exact signal reconstruction from highly incomplete frequency information," *IEEE Trans. Inform. Theory*, vol. 52, no. 2, pp. 489–509, Feb. 2006.

[13] J. A. Tropp and A. C. Gilbert, "Signal Recovery from Random Measurements via Orthogonal Matching Pursuit," *IEEE Trans. Inform. Theory*, vol. 53, no. 12, pp. 4655–4666, Dec. 2007.

[14] A. A. Lazar and L. T. Toth, "Perfect Recovery and Sensitivity Analysis of Time Encoded Bandlimited Signals," *IEEE Trans. Circuits Systems I*, vol. 51, no. 10, pp. 2060-2073, Oct. 2004.

[15] N. S. Jayant and A. E. Rosenberg, "The preference of slope overload to granularity in the delta modulation of speech," *Bell System Technical Journal*, vol. 50, no. 10, Dec. 1971.

[16] A. S. Alvarado and J. C. Principe, "From compressive to adaptive sampling of neural and ECG recordings," in *Proc. of IEEE ICASSP,* pp. 633-636, Apr. 2011.

[17] X. Chen, Z. Yu, S. Hoyos, B. M. Sadler and J. Silva-Martinez, "A sub-Nyquist rate sampling receiver exploiting compressive sensing," *IEEE Trans. Circuits Systems I*, vol. 58, no. 3, pp. 507-520, Mar. 2011.

[18] B. Wohlberg and P. Rodriguez, "An iteratively reweighted norm algorithm for minimization of total variation functionals," *IEEE Signal Proc. Letters*, vol. 14, no. 12, pp. 948-951, Dec. 2007.

[19] L. Rudin, S. Osher, and E. Fatemi, "Nonlinear total variation based noise removal algorithms," *Physica D* 60, 259 – 268, 1992.